Revista Brasileira de Cartografia
ISSN 1808-0936 | https://doi.org/10.14393/revbrascartogr
Sociedade Brasileira de Cartografia, Geodésia, Fotogrametria e Sensoriamento Remoto

Red Tide Detection and Chlorophyll-a Concentration Retrieval in Southeast Coast of Brazil

Detecção de Maré Vermelha e Estimativa da Concentração de Clorofila-a na Costa Sudeste do Brasil

Júlio César Pimenta dos Santos[1], Bruno Rech[2], Daniel Andrade Maciel[3], Cláudio Clemente Faria Barbosa[4], Áurea Maria Ciotti[5], Vitor Souza Martins[6], Rejane de Souza Paulino[7] e Evlyn Márcia Leão de Moraes Novo[8]

1 Instrumentation Lab for Aquatic Systems (LabISA), Earth Observation Coordination of National Institute for Space Research (INPE), São José dos Campos, Brazil. julio.santos@inpe.br;
ORCID: https://orcid.org/0000-0001-9194-6077
2 LabISA, Earth Observation Coordination of INPE, São José dos Campos, Brazil. bruno.rech@inpe.br;
ORCID: https://orcid.org/0000-0003-2787-2450
3 LabISA, Earth Observation Coordination of INPE, São José dos Campos, Brazil. daniel.maciel@inpe.br;
ORCID: https://orcid.org/0000-0003-4543-5908
4 LabISA, Earth Observation Coordination of INPE, São José dos Campos, Brazil. claudio.barbosa@inpe.br;
ORCID: https://orcid.org/0000-0002-3221-9774
5 Center for Marine Biology (CEBIMar) – University of São Paulo (USP) São Sebastião, SP, Brazil. ciotti@usp.br;
ORCID: https://orcid.org/0000-0001-7163-8819
6 Department of Agricultural & Biological Engineering, Mississippi State University, Starkville, MS, USA. vmartins@abe.msstate.edu;
ORCID: https://orcid.org/0000-0003-3802-0368
7 Department of Agricultural & Biological Engineering, Mississippi State University, Starkville, MS, USA. rdp282@msstate.edu;
ORCID: https://orcid.org/0000-0002-7295-8942
8 LabISA, Earth Observation Coordination of INPE, São José dos Campos, Brazil. evlyn.novo@inpe.br;
ORCID: https://orcid.org/0000-0002-1223-9276

Recebido: 08.2025 | Aceito: 10.2025

Abstract: We evaluated reflectance spectra and spectral features of a red tide event associated with high abundances of *Mesodinium rubrum*. The bloom was observed on the northern coast of the State of São Paulo between 12 and 25 January 2025, with hyperspectral ocean color satellite images. The diagnostic features of phytoplankton algae were observed near 610 nm and 705 nm, with a peak at 665 nm before decreasing. The Normalized Difference Red Tide (NDRT) was developed to map red tide occurrences. For the Bloom class, NDRT values are approximately 0.90, whereas for the No Bloom class, they range from 0.25 to 0.55. We also estimated chl-a concentration using different models: Normalized Difference Chlorophyll Index (NDCI) (0 – 60 mg/m^3), a method based on Two Bands Algorithm (2BDA) (0 – 275 mg/m^3), Algae Bloom Monitoring Application (AlgaeMAp) (0 - 1600 mg/m^3) and Ocean Color 4 (OC4) (0.35 – 0.65 mg/m^3).
Keywords: PRISMA. NDRT. Mesodinium rubrum. Bloom.

Resumo: Avaliamos espectros de reflectância e feições espectrais de um evento de maré vermelha associado a altas abundâncias de *Mesodinium rubrum*. A floração foi observada na costa norte do Estado de São Paulo entre 12 e 25 de janeiro de 2025, por meio de imagens hiperespectrais de satélite de cor do oceano. As feições diagnósticas do fitoplâncton foram observadas próximas a 610 nm e 705 nm, com um pico em 665 nm antes de decrescer. O Normalized Difference Red Tide (NDRT) foi desenvolvido para mapear ocorrências de maré vermelha. Para a classe Bloom, os valores de NDRT são aproximadamente 0,90, enquanto para a classe No Bloom variam de 0,25 a 0,55. Também estimamos a concentração de clorofila-a utilizando diferentes modelos: Normalized Difference Chlorophyll Index (NDCI) (0 – 60 mg/m³), um método baseado no Two Bands Algorithm (2BDA) (0 – 275 mg/m³), Algae Bloom Monitoring Application (AlgaeMAp) (0 – 1600 mg/m³) e Ocean Color 4 (OC4) (0,35 – 0,65 mg/m³).
Palavras-chave: PRISMA. NDRT. Mesodinium rubrum. Bloom.

1 INTRODUCTION

Red-appearance algal blooms, popularly called “red tides”, are caused by the proliferation of photosynthetic microscopic organisms that carry reddish pigments in their cells. These events have many ecological and economic implications and are easily perceived by people involved with touristic and fisheries activities, which need information for decision making about their safety (Burkholder et al., 2018). One of the major red-tide species is the mixotrophic ciliate *Mesodinium rubrum* (Johnson et al., 2016), that is reported to form blooms that can occur nearshore and extend for kilometers (Guzmán et al., 2016; Taylor et al., 1971).

Even though *M. rubrum* does not produce toxins, it is still considered a form of harmful algal blooms (HABs), as the decomposition of organic matter resulting from the decline of high concentrations may lead to hypoxia. In addition, *M. rubrum* is the main prey of dinoflagellates of the genus Dinophysis, a group of toxin-producing and HAB-forming microorganisms (Hansen et al., 2013). Consequently, the occurrence of *M. rubrum* blooms can facilitate Dinophysis blooms (Díaz et al., 2025), which may cause significant socio-economic and environmental impacts. Some species of Dinophysis produce okadaic acid, a toxin that accumulates in mussels and other marine organisms, causing severe gastrointestinal problems when consumed by humans (e.g., GUZMÁN et al., 2016).

Due to the risks to human health, impacts on seafood production, and environmental disturbances caused by HABs, their monitoring is crucial, and thus there is a need for accessible tools not only for detecting these events, but also for tracking their spatial and temporal distribution. Ocean color remote sensing has, therefore, proven to be a crucial tool that, when associated with in-situ sampling, can reveal the dominant organism present and the dynamics of the bloom in a given area (Cetinić et al., 2024).

Remote-sensing-based monitoring is facilitated by the public availability of data from high spatial resolution sensors such as the Sentinel-2 Multispectral Imager (S2/MSI), Sentinel-3 Ocean and Land Colour Instrument (S3/OLCI), and Hyperspectral Precursor of the Application Mission Hyperspectral Camera (HYC/PRISMA). The latter is part of a new generation of sensors that enable the assessment of aquatic systems with a spectral (dozens of bands) and spatial (30 m) resolution adequate for monitoring the intricate distribution of high concentrations of bloom-forming organisms, typically observed as patches. Algorithms based on hyperspectral data have been shown to outperform those based on multispectral data (HESTIR et al., 2015), leading to improved estimates of optically active constituents such as chlorophyll-a concentration (chl-a). However, the choice of the best algorithms, especially for detecting HABs in a given area, needs a systematic investigation that includes characterizing species occurrences in situ during reported events. To assesses the applicability of hyperspectral data to detect *M. rubrum* blooms in São Sebastião nearshore waters, in this study we evaluated the data registered by the HYC/PRISMA sensor during a *M. rubrum* bloom, assessing both the hyperspectral features and the changes in the spatial distribution of the observed patches. A new remote-sensing based index was also developed to provide a better separation of the *M. rubrum* blooms, based on their specific spectral features. In addition to the qualitative analysis, we also applied two widely used methods for chl-a estimation to understand quantitatively the increase in chl-a concentration caused by the blooms.

2 MATERIALS AND METHODS

2.1 Study area

The red tide event occurred in the northern littoral of the State of São Paulo, on the coast of São Sebastião and Ilhabela municipalities, including the marine protected area of the Alcatrazes archipelago, between 12 and 25 January 2025 (Figure 1). The occurrence of algal blooms in this region is not unprecedented, and the São Paulo Environmental Sanitation Technology Company has a contingency plan for the integrated management of HABs in the littoral (CETESB, 2021). It was in part motivated by HABs that occurred in 2014 and 2016, when the government embargoed the trade of seafood due to health risks (Mafra et al., 2019).

Figure 1 - S2/MSI true color image (01/20/2025) of the algal bloom event, and *M. rubrum* image from microscopy. True-color RGB: R(633nm), G(547nm), B(472nm). (from MACIEL et al., 2025).

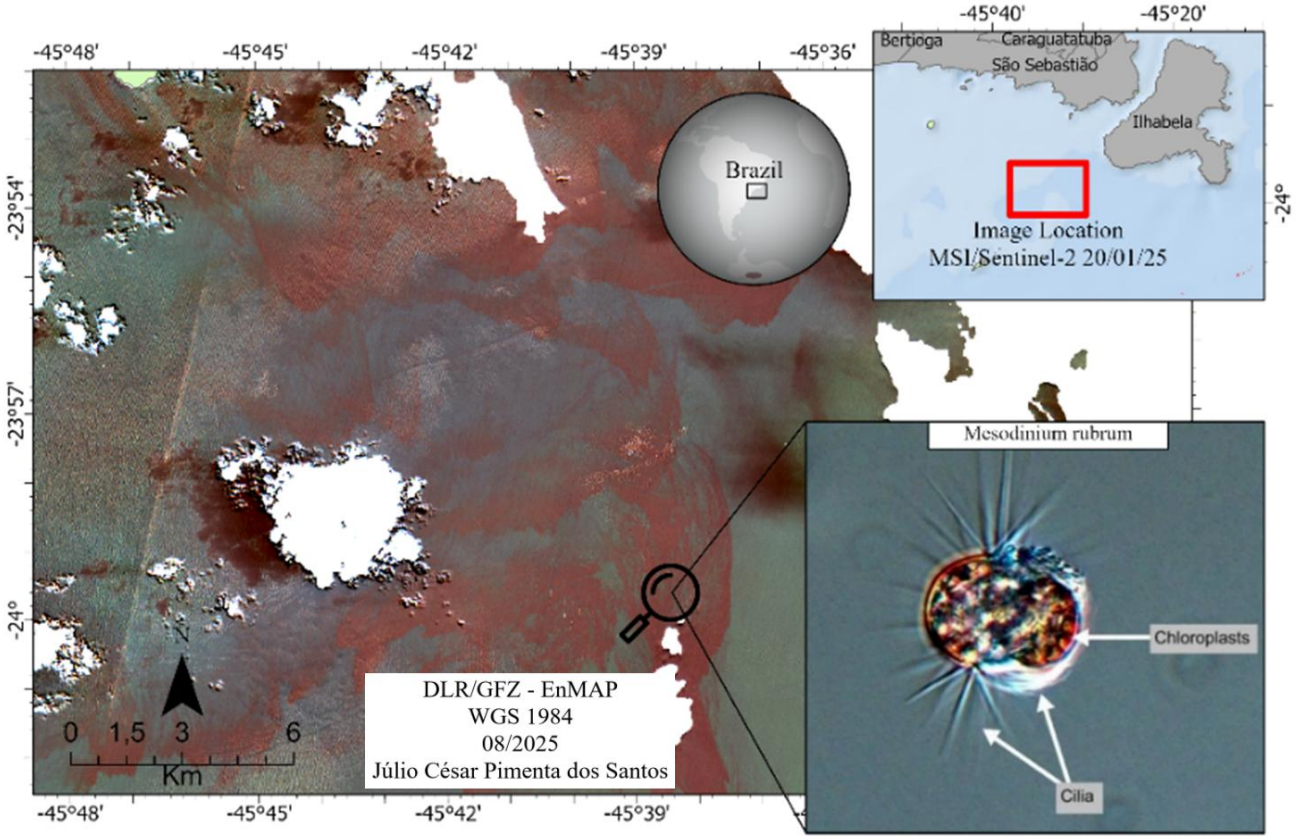

Source: Maciel et al., (2025).

2.2 Workflow

The workflow of this study was divided into two main steps to assess the occurrence of red tide in the study area (Figure 2). From hyperspectral satellite images obtained from PRISMA/HYC sensor, remote sensing reflectance (R_{rs}) spectra were extracted from samples of the Bloom and No Bloom classes. Then, the spectra was used as input for remote sensing models for estimating Chl-a. The extracted R_{rs} spectra were also used for the development of the Normalized Difference Red Tide (NDRT) index and to create a mapping of red tide occurrence (Figure 2).

Figure 2 - Flowchart of methodology and materials.

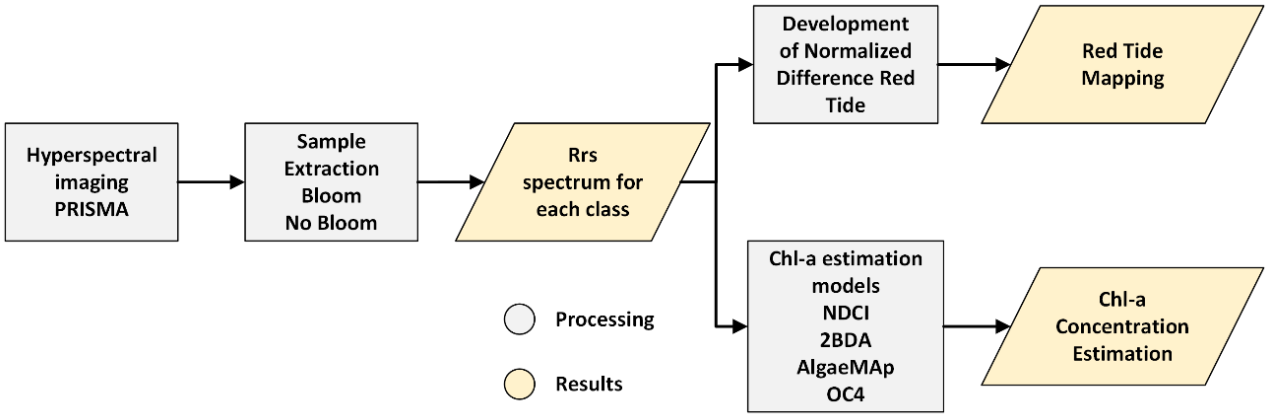

Source: Authors (2025).

2.3 Satellite data

The Hyperspectral Camera (HYC) onboard PRISMA has 66 spectral bands in the visible and near

infrared regions (VNIR, 400 to 1100 nm), and 174 spectral bands in the shortwave infrared region (SWIR, 920 to 2500 nm). The bandwidths vary from 9 to 15 nm, with a swath width of 30 km and 30-meter spatial resolution (ASI, 2023). Imagery acquisition is on demand. The sensor's viewing angle has a cyclical variation between -20° to +20° depending on the location and overpassing date (Bresciani et al., 2022).

Hyperspectral R_{rs} values were extracted from the PRISMA scene acquired on 20 January 2025, which was processed by the standard PRISMA atmospheric correction model (MODTRAN v6.0) and made available in R_{rs} (sr^{-1}) (Braga et al., 2022). Areas were selected visually through an RGB composition, then the spectra were extracted, and the median spectrum of the area (diameter of ~500 m) was calculated (Figure 3).

Figure 3 - HYC/PRISMA image and sample extraction area, in red area with Bloom and green area No Bloom. Bloom on 01/20/25. Located in the coastal area of São Paulo state, Brazil. True-color RGB: R(633nm), G(547nm), B(472nm).

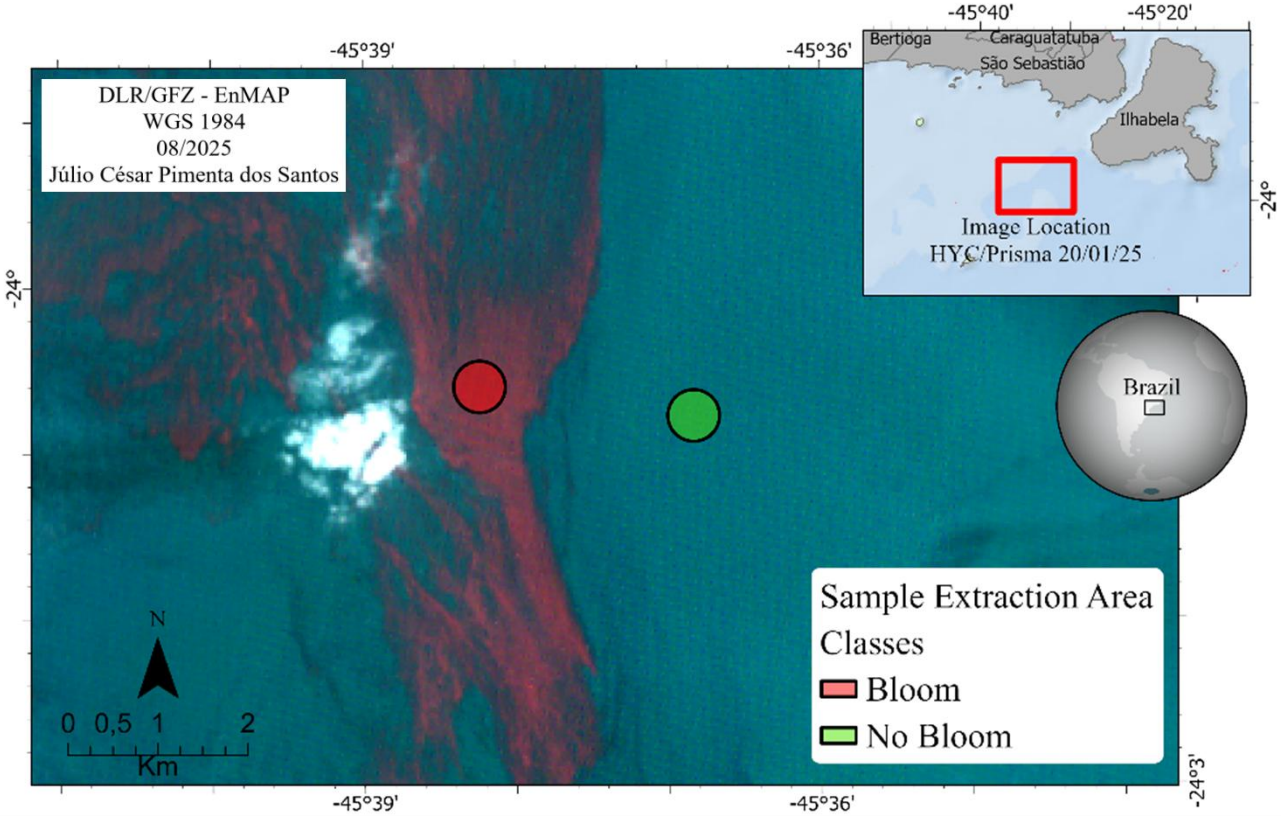

Source: Authors (2025).

2.4 Chl-a Concentration Estimation

Algae blooms are generally manifested in ocean color images as areas where estimated surface chl-a is high, as a proxy for phytoplankton biomass accumulation. We selected chl-a estimation models with straightforward applicability and high accuracy, which use spectral indices as a basis (Ogashawara et al., 2021); they were implemented using radiometric data from HYC/PRISMA. The Normalized Difference Chlorophyll Index (NDCI) was calculated based on Equation 1 and is frequently used in water quality studies (Mishra & Mishra, 2012). The Two Bands Algorithm (2BDA) is traditionally used in remote sensing for chl-a detection and estimation (Eq. 2), being a predecessor of other equations such as NDCI (Table 1) (Dall'Olmo & Gitelson, 2005). Two different NDCI-based algorithms previously developed for Brazilian inland eutrophic reservoirs were applied in the study site to evaluate their applicability: i) the algorithm developed by Augusto-Silva et al. (2014) in a eutrophic reservoir in Brazil (Funil Reservoir, Rio de Janeiro) (Equation 3); ii) The Algae Bloom Monitoring Application (AlgaeMAp) (Eq. 5) NDCI-based algorithm, that was developed in the eutrophic Waters of São Paulo reservoirs (Lobo et al., 2021).

The Equation 4 used in the 2BDA was developed in inland waters with bloom occurrence in the USA (Beck et al., 2016). The Ocean Color 4 (OC4) model was developed with oceanic data with a large spatial and temporal sampling (Eq. 6), but the samples concentrate below 20 mg/m^3 of Chl-a, generating a limitation

in the model for bloom occurrences (O'Reilly & Werdell, 2019).

Table 1 - Spectral index equations and Chl-a estimation models.

Name	Equation	N°
NDCI	$\mathrm{NDCI} = \frac{R_{\mathrm{rs}}(705) - R_{\mathrm{rs}}(665)}{R_{\mathrm{rs}}(705) + R_{\mathrm{rs}}(665)}$	(1)
2BDA	$2\mathrm{BDA} = \frac{R_{\mathrm{rs}}(705)}{R_{\mathrm{rs}}(665)}$	(2)
Chl-a estimation by NDCI	$[\text{chl-a}]_{\mathrm{NDCI}} = 54 \times \mathrm{NDCI} + 23.8$	(3)
Chl-a estimation by 2BDA	$[\text{chl-a}]_{2\mathrm{BDA}} = 56.316 \times (2\mathrm{BDA}) - 19.899$	(4)
AlgaeMAp model	$[\text{chl-a}]_{\mathrm{AlgaeMAp}} = 23.44 \times (\mathrm{NDCI} + 1)^{7.95}$	(5)
OC4	$x = \log 10\left[\frac{(max[R_{rs}(492), R_{rs}(490), R_{rs}(510)])}{R_{rs}(560)}\right]$ $y = 0.4254 - 3.2168x + 2.8691x^2 - 0.6263x^3 - 1.0933x^4$ $[\text{chl-a}]_{\mathrm{OC4}} = 10^y$	(6)

Source: (1)(Mishra & Mishra, 2012), (2)(Dall'Olmo & Gitelson, 2005), (3)(Augusto-Silva et al., 2014), (4)(Beck et al., 2016), (5)(Lobo et al., 2021) and (6)(O'Reilly & Werdell, 2019).

2.5 Development of Normalized Difference Red Tide

In the development of the Normalized Difference Red Tide (NDRT), the spectral features extracted from samples of the Bloom and No Bloom classes were used (Equation 7). The development of the NDRT was based on the spectral peak in R_{rs} (615) associated with *M. rubrum* scattering and the spectral depression at R_{rs} (539) attributable to absorption (Guzmán et al., 2016; Kyewalyanga et al., 2002). The detection of these features was made possible by the hyperspectral resolution of the HYC/PRISMA sensor; in multispectral sensors such as MSI/Sentinel-2, these features may not be discernible (Gernez et al., 2023).The difference in pigmentation between red tide events and other algal blooms was also considered. The primary objective of the NDRT is to assist in mapping and highlighting areas with and without red tide occurrence. The difference between the NDCI and the NDRT is that the NDCI maps different types of algal blooms, whereas the NDRT is specifically focused on red tides.

$$NDRT = \frac{R_{\mathrm{rs}}(615) - R_{\mathrm{rs}}(539)}{R_{\mathrm{rs}}(615) + R_{\mathrm{rs}}(539)} + 1 \quad (7)$$

3 RESULTS AND DISCUSSION

The main differences between the R_{rs} spectra from within and outside the blooms are in the peaks around 610 nm and 705 nm, both related to the algal bloom (Dierssen et al., 2015; Duan et al., 2007) (Figure 4). It is possible to observe that, for wavelengths not related to phytoplankton absorption/fluorescence, the spectra remain similar (e.g., 400-500 nm). In addition, it has another characteristic spectral feature related to Chl-a absorption that is used in both spectral indexes (i.e., NDCI and NDRT), being close to 665 nm, with a reduction in R_{rs} compared to the high features of 610 nm and 705 nm. (Duan et al., 2007).

 DOI: http://dx.doi.org/10.14393/rbcv77n0a-79283

Figure 4 - Median, maximum and minimum of HYC/PRISMA image samples, in red area with Bloom and green area No Bloom.

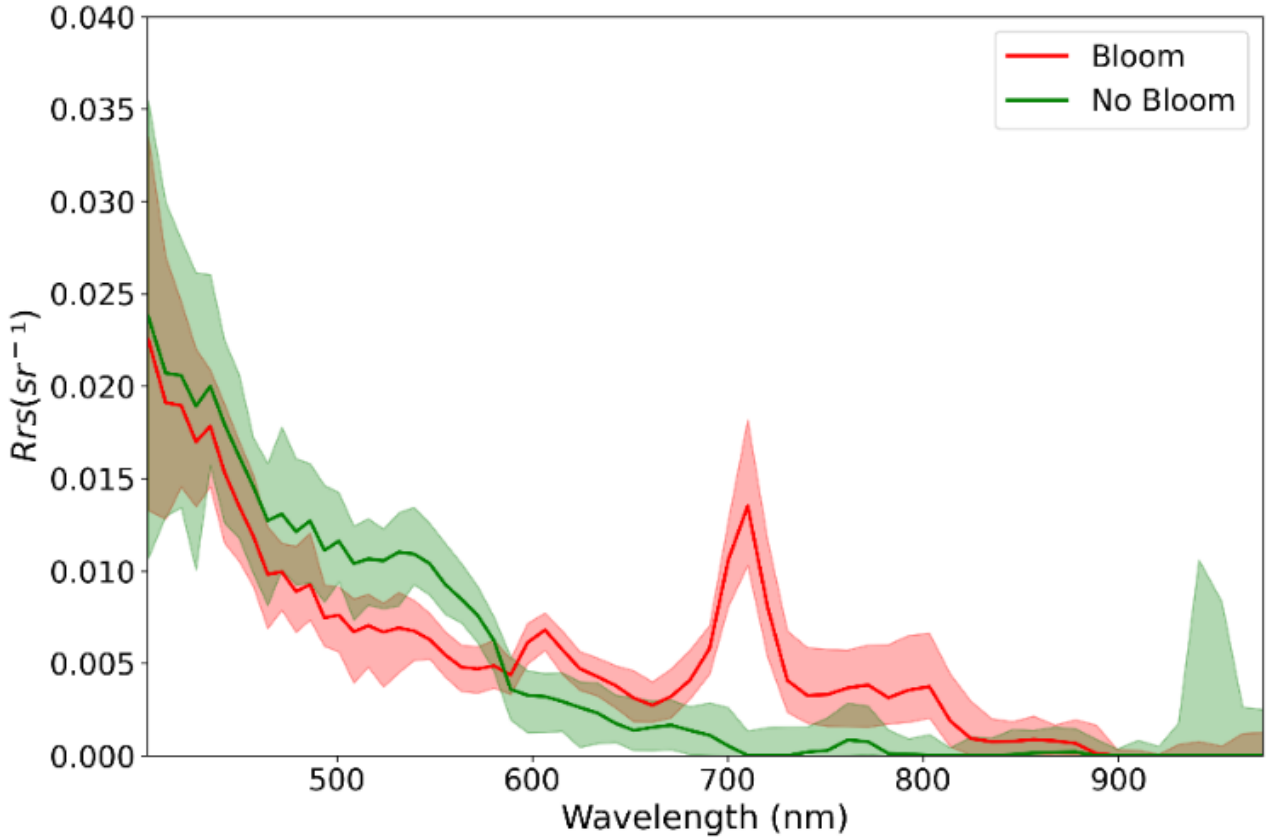

Source: Authors (2025).

Because NDCI is a normalized index, the results can only vary between -1 and 1, but 2BDA is a band ratio so it has values close to 5 (Figure 5). The NDCI results show values close to the two extremes, the area with Bloom with a mean of 0.75 and the No Bloom area with a mean of -1.00. For the 2BDA results, the areas with Bloom were close to 5 and the areas with No Bloom close to zero, in both equations the classes were well separated as expected.

Figure 5 - Spectral indices with samples from the HYC/Prisma sensor, in red area with Bloom and green area No Bloom.

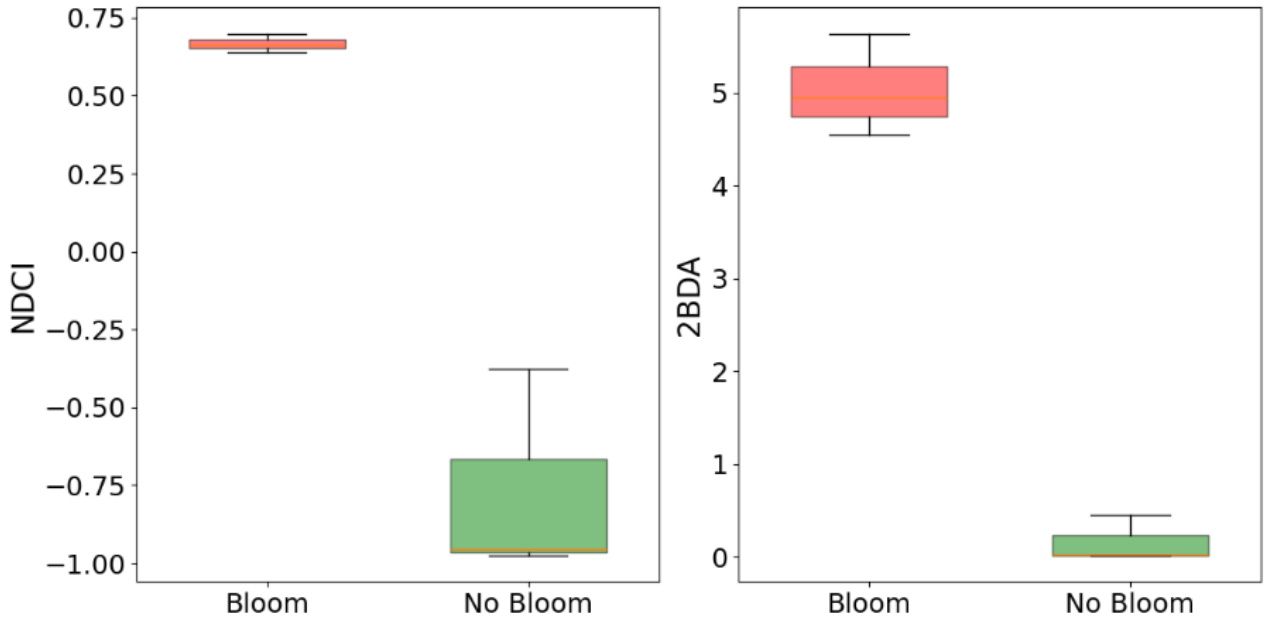

Source: Authors (2025).

The Chl-a estimates resulted in very different values between the methods, with NDCI Chl-a close to 60 mg/m^3, and 2BDA Chl-a close to 275 mg/m^3 in the areas with bloom. (Figure 6). The AlgaeMAp model reached the highest Chl-a estimate values, exceeding 1500 mg/m^3, which is close to the values found in-situ in bloom occurrences. The OC4 model underestimated the values in the area with Bloom, reaching lower values than those without bloom. The estimated values of Chl-a concentration for the No Bloom areas were close to zero, as expected. Unfortunately, due to the lack of Chl-a concentration data, it is not possible to validate the estimated values in this study, but the values estimated in this work are within the range of values from previous works (Ogashawara et al., 2021).

Figure 6 - Chl-a estimation with HYC/Prisma sensor samples, in red area with Bloom and green area No Bloom.

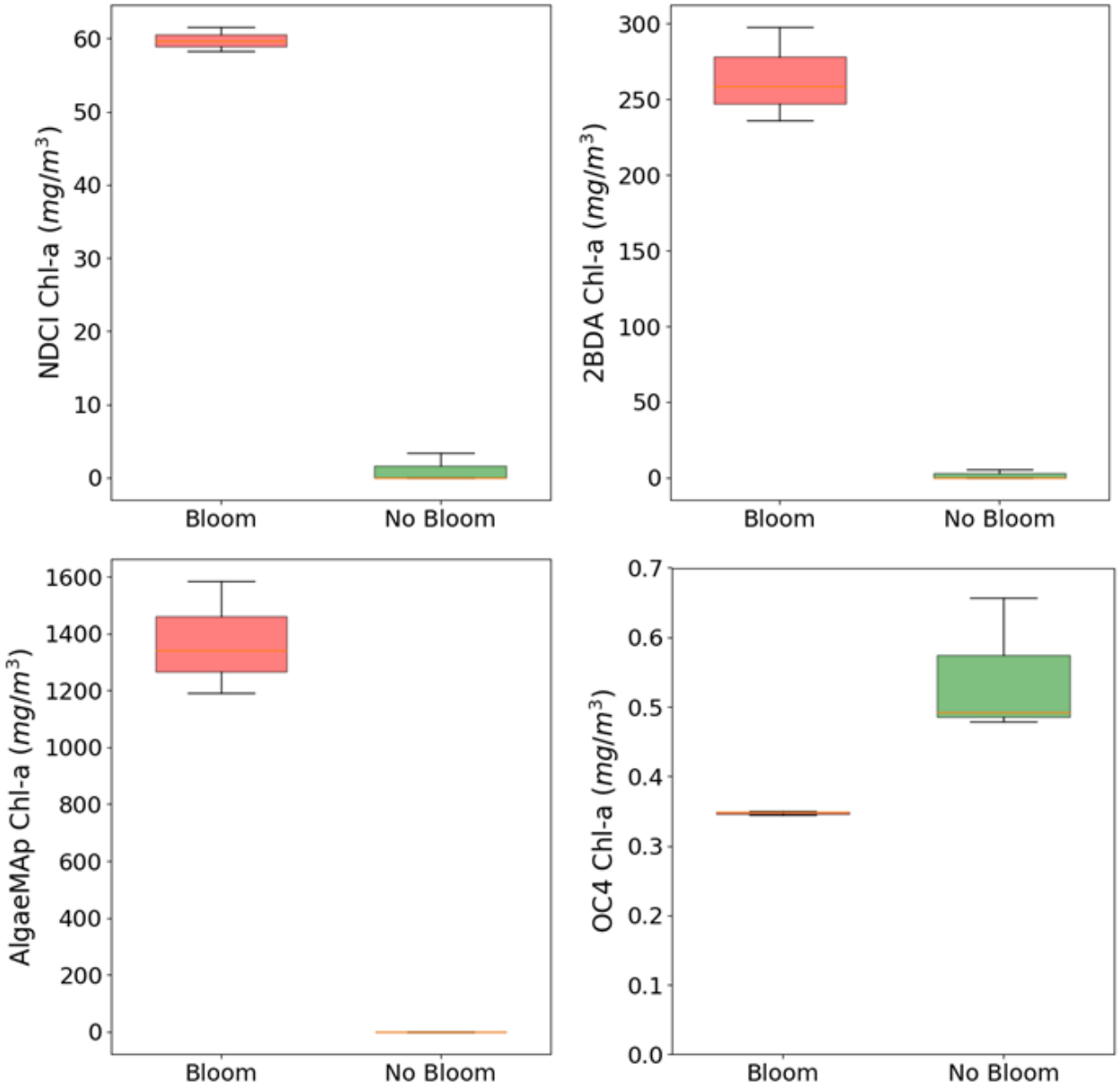

Source: Authors (2025).

Comparing the NDRT results between the Bloom and No Bloom classes, the classes do not overlap, demonstrating their separability (Figure 7). In the Bloom class, NDRT values are approximately 0.90, whereas in the No Bloom class, the values range between 0.25 and 0.55. In the red tide mapping using the NDRT, it was possible to highlight in red the areas of red tide occurrence, while the rest of the image was shown in blue (Figure 8). However, the NDRT may erroneously map areas that are not water, such as land, clouds, and shadows; therefore, it is necessary to use a water mask in conjunction.

Figure 7 - NDRT with HYC/Prisma sensor samples, in red area with Bloom and green area No Bloom.

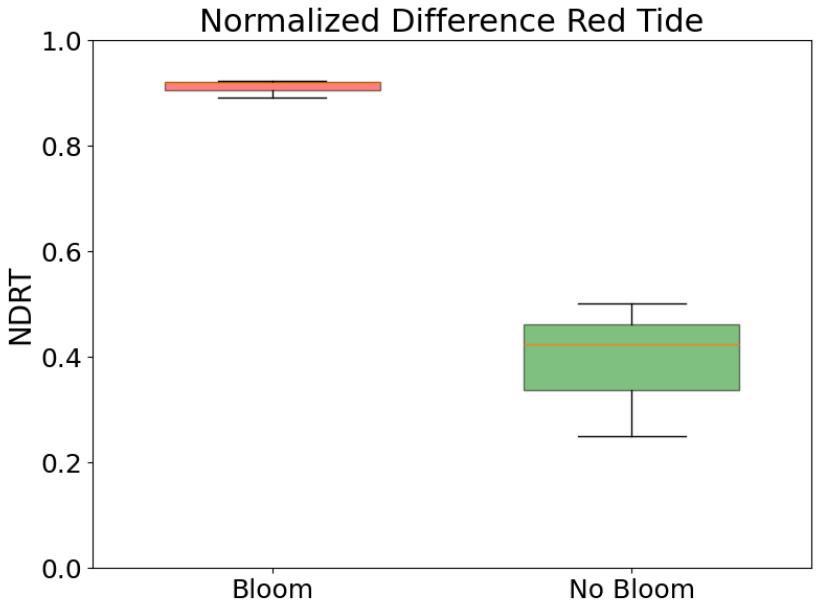

Source: Authors (2025).

Figure 8 - Comparison between RGB and NDRT in the HYC/PRISMA sensor image, in red area with Bloom and blue area No Bloom. True-color RGB: R(633nm), G(547nm), B(472nm).

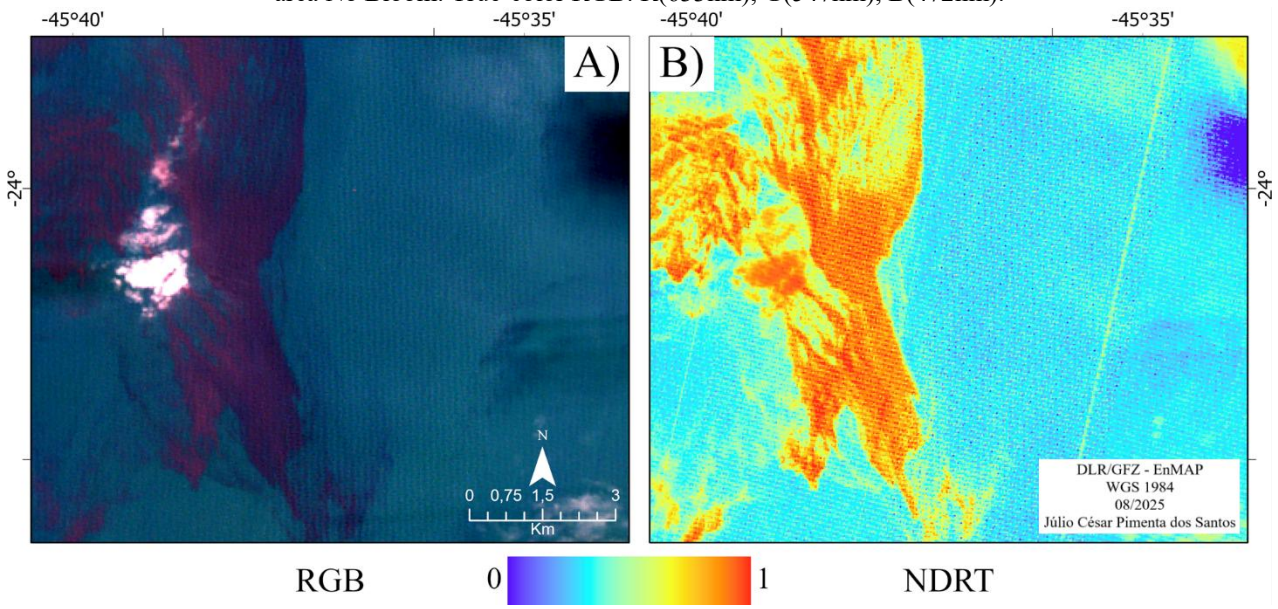

Source: Authors (2025).

4 CONCLUSIONS

In this work, we found the average spectrum and its main features of *Mesodinium rubrum*. We also estimated the concentration of Chl-a based on NDCI, 2BDA, AlgaeMAp and OC4. HYC/Prisma reproduced detailed features of M. *rubrum*, enabling the development of new Chl-a estimation models, making better use of the potential of hyperspectral data. The main features of bloom are close to 610 nm and 705 nm, with the highest values, and at 665 nm, a reduction of the values. The Normalized Difference Red Tide (NDRT) was developed to map red tide occurrences. For the Bloom class, NDRT values are approximately 0.90, whereas for the No Bloom class, they range from 0.25 to 0.55. The results of Chl-a concentrations have different ranges of NDCI (0 - 60 mg/m^3), 2BDA (0 - 275 mg/m^3), AlgaeMAp (0 - 1600 mg/m^3) and OC4 (0.35 – 0.65 mg/m^3) values. Among the models presented in this work, AlgaeMAp presented results with a greater range of values between areas with and without bloom, as described in previous works.

5 ACKNOWLEDGMENTS

This study was financed in part by the Conselho Nacional de Desenvolvimento Científico e Tecnológico (CNPq-Grants 306591/2022–7), São Paulo Research Foundation (FAPESP-Grants 2020/14613-8, 2021/13367-6, 2023/13904-7, 2024/06526-9, 2024/06636-9).

6 REFERENCES

ASI, Agenzia Spaziale Italiana. (2023). *PRISMA User Manual*. https://prisma.asi.it/missionselect/docs/PRISMA%20User%20Manual_Is1_3.pdf. Access: 10/03/2025

Beck, R., Zhan, S., Liu, H., Tong, S., Yang, B., Xu, M., Ye, Z., Huang, Y., Shu, S., Wu, Q., Wang, S., Berling, K., Murray, A., Emery, E., Reif, M., Harwood, J., Young, J., Nietch, C., Macke, D., … Su, H. (2016). Comparison of satellite reflectance algorithms for estimating chlorophyll-a in a temperate reservoir using coincident hyperspectral aircraft imagery and dense coincident surface observations. *Remote Sensing of Environment*, *178*, 15–30. https://doi.org/10.1016/j.rse.2016.03.002

Braga, F., Fabbretto, A., Vanhellemont, Q., Bresciani, M., Giardino, C., Scarpa, G. M., Manfè, G., Concha, J. A., & Brando, V. E. (2022). Assessment of PRISMA water reflectance using autonomous hyperspectral radiometry. *ISPRS Journal of Photogrammetry and Remote Sensing*, *192*, 99–114. https://doi.org/10.1016/j.isprsjprs.2022.08.009

Bresciani, M., Giardino, C., Fabbretto, A., Pellegrino, A., Mangano, S., Free, G., & Pinardi, M. (2022). Application of New Hyperspectral Sensors in the Remote Sensing of Aquatic Ecosystem Health: Exploiting PRISMA and DESIS for Four Italian Lakes. *Resources*, *11*(2), 8. https://doi.org/10.3390/resources11020008

Burkholder, J. M., Shumway, S. E., & Glibert, P. M. (2018). Food Web and Ecosystem Impacts of Harmful Algae. Em S. E. Shumway, J. M. Burkholder, & S. L. Morton (Org.), *Harmful Algal Blooms* (1º ed., p. 243–336). Wiley. https://doi.org/10.1002/9781118994672.ch7

CETESB. (2021). *PLANO DE CONTINGÊNCIA PARA GESTÃO INTEGRADA DE RISCOS ASSOCIADOS A FLORAÇÕES DE MICROALGAS TÓXICAS EM ÁGUAS DO LITORAL PAULISTA*. https://cetesb.sp.gov.br/wp-content/uploads/sites/24/2023/08/Plano-Contigencia-para-Gestao-Integrada-de-Riscos-Associados-a-Floracoes-de-Microalgas-Toxicas-em-Aguas-do-Litoral-Paulista.pdf

Cetinić, I., Rousseaux, C. S., Carroll, I. T., Chase, A. P., Kramer, S. J., Werdell, P. J., Siegel, D. A., Dierssen, H. M., Catlett, D., Neeley, A., Soto Ramos, I. M., Wolny, J. L., Sadoff, N., Urquhart, E., Westberry, T. K., Stramski, D., Pahlevan, N., Seegers, B. N., Sirk, E., … Sayers, M. (2024). Phytoplankton composition from sPACE: Requirements, opportunities, and challenges. *Remote Sensing of Environment*, *302*, 113964. https://doi.org/10.1016/j.rse.2023.113964

Dall'Olmo, G., & Gitelson, A. A. (2005). Effect of bio-optical parameter variability on the remote estimation of chlorophyll-a concentration in turbid productive waters: Experimental results. *Applied Optics*, *44*(3), 412. https://doi.org/10.1364/AO.44.000412

Díaz, P. A., Baldrich, Á. M., Rodríguez, F., Díaz, M., Álvarez, G., Pérez-Santos, I., Schwerter, C., Rodríguez-Villegas, C., Carbonell, P., Cantarero, B., López, L., & Reguera, B. (2025). *Mesodinium–Dinophysis* encounters: Temporal and spatial constraints on *Dinophysis* blooms. *Journal of Plankton Research*, *47*(2), fbae068. https://doi.org/10.1093/plankt/fbae068

Dierssen, H., McManus, G. B., Chlus, A., Qiu, D., Gao, B.-C., & Lin, S. (2015). Space station image captures a red tide ciliate bloom at high spectral and spatial resolution. *Proceedings of the National Academy of Sciences*, *112*(48), 14783–14787. https://doi.org/10.1073/pnas.1512538112

Duan, H., Zhang, Y., Zhang, B., Song, K., & Wang, Z. (2007). Assessment of Chlorophyll-a Concentration and Trophic State for Lake Chagan Using Landsat TM and Field Spectral Data. *Environmental Monitoring and Assessment*, *129*(1–3), 295–308. https://doi.org/10.1007/s10661-006-9362-y

Gernez, P., Zoffoli, M. L., Lacour, T., Fariñas, T. H., Navarro, G., Caballero, I., & Harmel, T. (2023). The

many shades of red tides: Sentinel-2 optical types of highly-concentrated harmful algal blooms. *Remote Sensing of Environment*, *287*, 113486. https://doi.org/10.1016/j.rse.2023.113486

Gruber, T., & Willberg, M. (2019). Signal and error assessment of GOCE-based high resolution gravity field models. *Journal of Geodetic Science*, *9*(1), 71–86. https://doi.org/10.1515/jogs-2019-0008

Guzmán, L., Varela, R., Muller-Karger, F., & Lorenzoni, L. (2016). Bio-optical characteristics of a red tide induced by Mesodinium rubrum in the Cariaco Basin, Venezuela. *Journal of Marine Systems*, *160*, 17–25. https://doi.org/10.1016/j.jmarsys.2016.03.015

Hansen, P. J., Nielsen, L. T., Johnson, M., Berge, T., & Flynn, K. J. (2013). Acquired phototrophy in Mesodinium and Dinophysis – A review of cellular organization, prey selectivity, nutrient uptake and bioenergetics. *Harmful Algae*, *28*, 126–139. https://doi.org/10.1016/j.hal.2013.06.004

Hestir, E. L., Brando, V. E., Bresciani, M., Giardino, C., Matta, E., Villa, P., & Dekker, A. G. (2015). Measuring freshwater aquatic ecosystems: The need for a hyperspectral global mapping satellite mission. *Remote Sensing of Environment*, *167*, 181–195. https://doi.org/10.1016/j.rse.2015.05.023

Kyewalyanga, M., Sathyendranath, S., & Platt, T. (2002). Effect of Mesodinium rubrum (= Myrionecta rubra) on the action and absorption spectra of phytoplankton in a coastal marine inlet. *Journal of Plankton Research*, *24*(7), 687–702. https://doi.org/10.1093/plankt/24.7.687

Lobo, F. D. L., Nagel, G. W., Maciel, D. A., Carvalho, L. A. S. D., Martins, V. S., Barbosa, C. C. F., & Novo, E. M. L. D. M. (2021). AlgaeMAp: Algae Bloom Monitoring Application for Inland Waters in Latin America. *Remote Sensing*, *13*(15), 2874. https://doi.org/10.3390/rs13152874

Maciel, D. A., Rech, B., Santos, J. C. P., Paulino, R., Martins, V. S., Novo, E., Ciotti, Á., & Barbosa, C. (2025). *NOTA TÉCNICA CONJUNTA LabISA/INPE, CEBIMAR/USP E GCER/MISSISSIPPI STATE UNIVERSITY - "MARÉ VERMELHA" NAS PRAIAS DE SÃO SEBASTIÃO E ILHABELA EM JANEIRO DE 2025*. https://www.gov.br/inpe/pt-br/assuntos/ultimas-noticias/copy_of_NotatcnicaLabISA.pdf

Mafra, L. L., Nolli, P. K. W., Mota, L. E., Domit, C., Soeth, M., Luz, L. F. G., Sobrinho, B. F., Leal, J. G., & Di Domenico, M. (2019). Multi-species okadaic acid contamination and human poisoning during a massive bloom of Dinophysis acuminata complex in southern Brazil. *Harmful Algae*, *89*, 101662. https://doi.org/10.1016/j.hal.2019.101662

Mishra, S., & Mishra, D. R. (2012). Normalized difference chlorophyll index: A novel model for remote estimation of chlorophyll-a concentration in turbid productive waters. *Remote Sensing of Environment*, *117*, 394–406. https://doi.org/10.1016/j.rse.2011.10.016

Ogashawara, I., Kiel, C., Jechow, A., Kohnert, K., Ruhtz, T., Grossart, H.-P., Hölker, F., Nejstgaard, J. C., Berger, S. A., & Wollrab, S. (2021). The Use of Sentinel-2 for Chlorophyll-a Spatial Dynamics Assessment: A Comparative Study on Different Lakes in Northern Germany. *Remote Sensing*, *13*(8), 1542. https://doi.org/10.3390/rs13081542

O'Reilly, J. E., & Werdell, P. J. (2019). Chlorophyll algorithms for ocean color sensors—OC4, OC5 & OC6. *Remote Sensing of Environment*, *229*, 32–47. https://doi.org/10.1016/j.rse.2019.04.021

Taylor, F. J. R., Blackbourn, D. J., & Blackbourn, J. (1971). The Red-Water Ciliate *Mesodinium rubrum* and its "Incomplete Symbionts": A Review Including New Ultrastructural Observations. *Journal of the Fisheries Research Board of Canada*, *28*(3), 391–407. https://doi.org/10.1139/f71-052

Conflicts of Interest

The authors declare no conflicts of interest.

 DOI: http://dx.doi.org/10.14393/rbcv77n0a-79283

Biography of the main author

Júlio César Pimenta dos Santos is an Environmental and Sanitary Engineer graduated from the University of Vale do Paraíba (UNIVAP). He holds a Master's degree and is currently a Ph.D. candidate in Remote Sensing at the National Institute for Space Research (INPE). His research focuses on the analysis of multispectral and hyperspectral remote sensing data applied to inland water bodies, with an emphasis on the State of São Paulo, Brazil.